# Numerical Investigation for Unsteady Heat Conduction Problems of Anisotropic Trigonometrically Graded Materials

Mohammad Ivan Azis*

*Abstract*—**Numerical solutions for unsteady problems governed by a Laplacian type equation with trigonometrically varying coefficients for anisotropic inhomogeneous media are sought using a mixed Laplace transform and boundary element method. Several examples for anisotropic quadratically graded media are considered. The results demonstrate ease of implementation and accuracy of the method.**

*Index Terms*—**numerical solutions, heat conduction problems, anisotropic FGMs, boundary element method, Laplace transforms**

## I. Introduction

We will consider initial boundary value problems governed by a Laplace type equation with variable coefficients of the form

$$\frac{\partial}{\partial x_i}\left[\kappa_{ij}\left(\mathbf{x}\right)\frac{\partial T\left(\mathbf{x},t\right)}{\partial x_j}\right]=\psi\left(\mathbf{x}\right)\frac{\partial T\left(\mathbf{x},t\right)}{\partial t}\quad i,j=1,2 \tag{1}$$

where the coefficients $[\kappa_{ij}]$ is a symmetric matrix with positive determinant, and summation convention holds for repeated indices so that explicitly equation (1) takes the form

$$\frac{\partial}{\partial x_1}\left(\kappa_{11}\frac{\partial T}{\partial x_1}\right)+\frac{\partial}{\partial x_1}\left(\kappa_{12}\frac{\partial T}{\partial x_2}\right)+\frac{\partial}{\partial x_2}\left(\kappa_{12}\frac{\partial T}{\partial x_1}\right)+\frac{\partial}{\partial x_2}\left(\kappa_{22}\frac{\partial T}{\partial x_2}\right)=\psi\frac{\partial c}{\partial t}$$

Equation (1) is usually used to model heat conduction problems (see for examples [1]–[4])), where $T$ is the temperature, $\kappa_{ij}$ is the anisotropic conductivity, and $\psi$ is the rate of change.

In recent years, there has been a growing interest in functionally graded materials (FGMs), with many studies focusing on their applications in various fields. FGMs are artificial materials that exhibit characteristics which are mathematically described as varying with both time and position, making Equation (1) particularly relevant for their study. These materials are created with specific practical objectives in mind, as evidenced by previous research (see, for example, [5], [6]), thus emphasizing the importance of solving Equation (1) in the context of FGMs.

Recently a number of authors had been working on the Laplace equation to find its solutions. However the works mainly focus on problems of isotropic homogeneous materials. For example, Yang et al. [3] investigated steady nonlinear heat conduction problems of homogeneous isotropic materials and solved them using a radial integration boundary element method. Guo et al [7] considered transient heat conduction problems of isotropic and homogeneous media and solved them using a combined Laplace transform and multiple reciprocity boundary face method. In [8] Fu et al. examined a boundary knot method used to find numerical solutions to problems of homogeneous isotropic media governed by a three-dimensional transient heat conduction with a source term. In [9] solutions of a Laplace type equation in unbounded domains are discussed.

Boundary element method (BEM) and other numerical methods have been effectively used to find solutions to problems related to functionally graded materials. However, for inhomogeneous materials, the lack of fundamental solutions for equations with variable coefficients makes it difficult to use these methods. Some progress of solving problems for inhomogeneous media using various techniques has been done. In [10] the authors investigated finite difference solutions of unsteady diffusion-convection problems for heterogeneous media. In [11] the authors studied the analytical solutions to a transient heat conduction equation of variable coefficients with a source term for a functionally graded orthotropic strip (FGOS). In this study, the inhomogeneity of the FGOS is simplified to be functionally graded in the $x$ variable only. In [12] the authors worked on finding numerical solutions to nonlinear transient heat conduction problems for anisotropic quadratically graded materials using a boundary domain element method. Several authors have conducted studies on equations with constant-plus-variable coefficients (see for example [13], [14], [15], [16], [17], [18]). By representing the variable coefficients as a sum of constant and variable coefficients, the derived integral equation will contain both boundary and domain integrals. The constant coefficient term will contribute boundary integrals since fundamental solutions are available, while the variable coefficient term will result in domain integrals.

The reduction to constant coefficients equation is a useful method for transforming variable coefficients equations into constant coefficients equations, which preserves the boundary-only integral equation. Researchers such as Azis and colleagues have been using this technique to solve steady-state problems for various types of governing equations, including the Helmholtz equation [19], modified Helmholtz equation [20], diffusion-convection equation [21], Laplace type equation [22], and diffusion-convection-reaction equation [23], for anisotropic inhomogeneous media. They have also investigated other classes of inhomogeneity functions for functionally graded materials that differ from

Manuscript received May 6, 2023; revised September 11, 2023.
*M. I. Azis is a professor at the Department of Mathematics, Hasanuddin University, Makassar, INDONESIA. (Corresponding author. Phone: +62811466230; e-mail: ivan@unhas.ac.id)

the class of constant-plus-variable coefficients, as reported in their papers.

This study is aimed to extend the recent works in [22] for steady anisotropic Laplace type equation with spatially variable coefficients of the form

$$\frac{\partial}{\partial x_i}\left[\kappa_{ij}(\mathbf{x})\frac{\partial T(\mathbf{x},t)}{\partial x_j}\right]=0$$

to unsteady anisotropic Laplace type equation with spatially variable coefficients of the form (1).

## II. The initial-boundary value problem

The goal is to find solutions and their derivatives of equation (1) with respect to a Cartesian frame $Ox_1x_2$. These solutions are valid for time $t \geq 0$ in a region $\Omega$ in $R^2$ with a boundary $\partial\Omega$ consisting of a finite number of piecewise smooth closed curves. On $\partial\Omega_1$ the dependent variable $T(\mathbf{x},t)$ $(\mathbf{x}=(x_1,x_2))$ is specified and on $\partial\Omega_2$

$$P(\mathbf{x},t)=\kappa_{ij}(\mathbf{x})\frac{\partial T(\mathbf{x},t)}{\partial x_i}n_j \tag{2}$$

is specified where $\partial\Omega=\partial\Omega_1\cup\partial\Omega_2$ and $\mathbf{n}=(n_1,n_2)$ denotes the outward pointing normal to $\partial\Omega$. The initial condition is taken to be

$$T(\mathbf{x},0)=0 \tag{3}$$

## III. The boundary integral equation

The coefficients $\kappa_{ij},\psi$ are required to take the form

$$\kappa_{ij}(\mathbf{x}) = \overline{\kappa}_{ij}g(\mathbf{x}) \tag{4}$$
$$\psi(\mathbf{x}) = \overline{\psi}g(\mathbf{x}) \tag{5}$$

where the $\overline{\kappa}_{ij},\overline{\psi}$ are constants and $g$ is a differentiable function of $\mathbf{x}$. Further we assume that the coefficients $\kappa_{ij}(\mathbf{x})$ and $\psi(\mathbf{x})$ are trigonometrically graded by taking $g(\mathbf{x})$ as an trigonometric function

$$g(\mathbf{x})=\left[A\cos(c_0+c_ix_i)+B\sin(c_0+c_ix_i)\right]^2 \tag{6}$$

where $A,B,c_0$ and $c_i$ are constants. Therefore if

$$\overline{\kappa}_{ij}c_ic_j+\lambda=0 \tag{7}$$

then (6) satisfies

$$\overline{\kappa}_{ij}\frac{\partial^2 g^{1/2}}{\partial x_i\partial x_j}-\lambda g^{1/2}=0 \tag{8}$$

Use of (4)-(5) in (1) yields

$$\overline{\kappa}_{ij}\frac{\partial}{\partial x_i}\left(g\frac{\partial T}{\partial x_j}\right)=\overline{\psi}g\frac{\partial T}{\partial t} \tag{9}$$

Let

$$T(\mathbf{x},t)=g^{-1/2}(\mathbf{x})\,\sigma(\mathbf{x},t) \tag{10}$$

therefore substitution of (4) and (10) into (2) gives

$$P(\mathbf{x},t)=-P_g(\mathbf{x})\,\sigma(\mathbf{x},t)+g^{1/2}(\mathbf{x})\,P_\sigma(\mathbf{x},t) \tag{11}$$

where

$$P_g(\mathbf{x})=\overline{\kappa}_{ij}\frac{\partial g^{1/2}}{\partial x_j}n_i \qquad P_\sigma(\mathbf{x})=\overline{\kappa}_{ij}\frac{\partial\sigma}{\partial x_j}n_i$$

Also, (9) may be written in the form

$$\overline{\kappa}_{ij}\frac{\partial}{\partial x_i}\left[g\frac{\partial\left(g^{-1/2}\sigma\right)}{\partial x_j}\right]=\overline{\psi}g\frac{\partial\left(g^{-1/2}\sigma\right)}{\partial t}$$

which can be simplified

$$\overline{\kappa}_{ij}\frac{\partial}{\partial x_i}\left(g^{1/2}\frac{\partial\sigma}{\partial x_j}+g\sigma\frac{\partial g^{-1/2}}{\partial x_j}\right)=\overline{\psi}g^{1/2}\frac{\partial\sigma}{\partial t}$$

Use of the identity

$$\frac{\partial g^{-1/2}}{\partial x_i}=-g^{-1}\frac{\partial g^{1/2}}{\partial x_i}$$

implies

$$\overline{\kappa}_{ij}\frac{\partial}{\partial x_i}\left(g^{1/2}\frac{\partial\sigma}{\partial x_j}-\sigma\frac{\partial g^{1/2}}{\partial x_j}\right)=\overline{\psi}g^{1/2}\frac{\partial\sigma}{\partial t}$$

Rearranging and neglecting the zero terms yield

$$g^{1/2}\overline{\kappa}_{ij}\frac{\partial^2\sigma}{\partial x_i\partial x_j}-\sigma\overline{\kappa}_{ij}\frac{\partial^2 g^{1/2}}{\partial x_i\partial x_j}=\overline{\psi}g^{1/2}\frac{\partial\sigma}{\partial t}$$

Equation (8) then implies

$$\overline{\kappa}_{ij}\frac{\partial^2\sigma}{\partial x_i\partial x_j}-\lambda\sigma=\overline{\psi}\frac{\partial\sigma}{\partial t} \tag{12}$$

Taking the Laplace transform of (10), (11), (12) and applying the initial condition (3) we obtain

$$\sigma^*(\mathbf{x},s)=g^{1/2}(\mathbf{x})\,T^*(\mathbf{x},s) \tag{13}$$

$$P_{\sigma^*}(\mathbf{x},s)=\left[P^*(\mathbf{x},s)+P_g(\mathbf{x})\,\sigma^*(\mathbf{x},s)\right]g^{-1/2}(\mathbf{x}) \tag{14}$$

$$\overline{\kappa}_{ij}\frac{\partial^2\sigma^*}{\partial x_i\partial x_j}-\left(\lambda+s\overline{\psi}\right)\sigma^*=0 \tag{15}$$

where $s$ is the variable of the Laplace-transformed domain.

A boundary integral equation for the solution of (15) is given in the form

$$\begin{aligned}\eta(\mathbf{x}_0)\,\sigma^*(\mathbf{x}_0,s)=&\int_{\partial\Omega}\left[\Gamma(\mathbf{x},\mathbf{x}_0)\,\sigma^*(\mathbf{x},s)\right.\\&\left.-\Phi(\mathbf{x},\mathbf{x}_0)\,P_{\sigma^*}(\mathbf{x},s)\right]dS(\mathbf{x})\end{aligned} \tag{16}$$

where $\mathbf{x}_0=(a,b)$, $\eta=0$ if $(a,b)\notin\Omega\cup\partial\Omega$, $\eta=1$ if $(a,b)\in\Omega$, $\eta=\frac{1}{2}$ if $(a,b)\in\partial\Omega$ and $\partial\Omega$ has a continuously turning tangent at $(a,b)$. The so called fundamental solution $\Phi$ in (16) is any solution of the equation

$$\overline{\kappa}_{ij}\frac{\partial^2\Phi}{\partial x_i\partial x_j}-\left(\lambda+s\overline{\psi}\right)\Phi=\delta(\mathbf{x}-\mathbf{x}_0)$$

and the $\Gamma$ is given by

$$\Gamma(\mathbf{x},\mathbf{x}_0)=\overline{\kappa}_{ij}\frac{\partial\Phi(\mathbf{x},\mathbf{x}_0)}{\partial x_j}n_i$$

where $\delta$ is the Dirac delta function. For two-dimensional problems $\Phi$ and $\Gamma$ are given by

$$\Phi(\mathbf{x},\mathbf{x}_0) = \begin{cases}\frac{K}{2\pi}\ln R & \text{if } \lambda+s\overline{\psi}=0\\ \frac{\imath K}{4}H_0^{(2)}(\omega R) & \text{if } \lambda+s\overline{\psi}<0\\ \frac{-K}{2\pi}K_0(\omega R) & \text{if } \lambda+s\overline{\psi}>0\end{cases}$$

$$\Gamma(\mathbf{x},\mathbf{x}_0) = \begin{cases}\frac{K}{2\pi}\frac{1}{R}\overline{\kappa}_{ij}\frac{\partial R}{\partial x_j}n_i\\ \frac{-\imath K\omega}{4}H_1^{(2)}(\omega R)\,\overline{\kappa}_{ij}\frac{\partial R}{\partial x_j}n_i\\ \frac{K\omega}{2\pi}K_1(\omega R)\,\overline{\kappa}_{ij}\frac{\partial R}{\partial x_j}n_i\end{cases}$$

$$\begin{cases}\text{if } \lambda+s\overline{\psi}=0\\ \text{if } \lambda+s\overline{\psi}<0\\ \text{if } \lambda+s\overline{\psi}>0\end{cases} \tag{17}$$

where

$$\begin{aligned} K &= \ddot{\tau}/D \\ \omega &= \sqrt{|\lambda + s\overline{\psi}|/D} \\ D &= \left[\overline{\kappa}_{11} + 2\overline{\kappa}_{12}\dot{\tau} + \overline{\kappa}_{22}\left(\dot{\tau}^2 + \ddot{\tau}^2\right)\right]/2 \\ R &= \sqrt{(\dot{x}_1 - \dot{a})^2 + (\dot{x}_2 - \dot{b})^2} \\ \dot{x}_1 &= x_1 + \dot{\tau}x_2 \\ \dot{a} &= a + \dot{\tau}b \\ \dot{x}_2 &= \ddot{\tau}x_2 \\ \dot{b} &= \ddot{\tau}b \end{aligned}$$

where $\dot{\tau}$ and $\ddot{\tau}$ are respectively the real and the positive imaginary parts of the complex root $\tau$ of the quadratic

$$\overline{\kappa}_{11} + 2\overline{\kappa}_{12}\tau + \overline{\kappa}_{22}\tau^2 = 0$$

and $H_0^{(2)}$, $H_1^{(2)}$ denote the Hankel function of second kind and order zero and order one respectively. $K_0$, $K_1$ denote the modified Bessel function of order zero and order one respectively, $\imath$ represents the square root of minus one. The derivatives $\partial R/\partial x_j$ needed for the calculation of the $\Gamma$ in (17) are given by

$$\begin{aligned} \frac{\partial R}{\partial x_1} &= \frac{1}{R}\left(\dot{x}_1 - \dot{a}\right) \\ \frac{\partial R}{\partial x_2} &= \dot{\tau}\left[\frac{1}{R}\left(\dot{x}_1 - \dot{a}\right)\right] + \ddot{\tau}\left[\frac{1}{R}\left(\dot{x}_2 - \dot{b}\right)\right] \end{aligned}$$

Use of (13) and (14) in (16) yields

$$\begin{aligned} \eta g^{1/2}T^* &= \int_{\partial\Omega}\left[\left(g^{1/2}\Gamma - P_g\Phi\right)T^*\right. \\ &\quad \left. - \left(g^{-1/2}\Phi\right)P^*\right]dS \end{aligned} \tag{18}$$

This equation provides a boundary integral equation for determining $T^*$ and its derivatives at all points of $\Omega$.

After solving the boundary integral equation in the Laplace transform variable using a standard boundary element method, the solutions and their derivatives in the Laplace transform variable are obtained. The Stehfest formula is then used for a numerical Laplace transform inversion to find the solutions and their derivatives in the original time variable. The obtained solutions and their derivatives are for the original variable $t$, which were previously transformed to the Laplace transform variable $s$. The Stehfest formula is

$$\begin{aligned} T(\mathbf{x},t) &\simeq \frac{\ln 2}{t}\sum_{m=1}^{N} V_m T^*(\mathbf{x},s_m) \\ \frac{\partial T(\mathbf{x},t)}{\partial x_1} &\simeq \frac{\ln 2}{t}\sum_{m=1}^{N} V_m \frac{\partial T^*(\mathbf{x},s_m)}{\partial x_1} \\ \frac{\partial T(\mathbf{x},t)}{\partial x_2} &\simeq \frac{\ln 2}{t}\sum_{m=1}^{N} V_m \frac{\partial T^*(\mathbf{x},s_m)}{\partial x_2} \end{aligned} \tag{19}$$

where

$$\begin{aligned} s_m &= \frac{\ln 2}{t}m \\ V_m &= (-1)^{\frac{N}{2}+m} \times \\ &\sum_{k=\left[\frac{m+1}{2}\right]}^{\min\left(m,\frac{N}{2}\right)} \frac{k^{N/2}(2k)!}{\left(\frac{N}{2}-k\right)!k!(k-1)!(m-k)!(2k-m)!} \end{aligned}$$

TABLE I
VALUES OF $V_m$ OF THE STEHFEST FORMULA

| $V_m$ | $N=6$ | $N=8$ | $N=10$ | $N=12$ |
|---|---|---|---|---|
| $V_1$ | 1 | −1/3 | 1/12 | −1/60 |
| $V_2$ | −49 | 145/3 | −385/12 | 961/60 |
| $V_3$ | 366 | −906 | 1279 | −1247 |
| $V_4$ | −858 | 16394/3 | −46871/3 | 82663/3 |
| $V_5$ | 810 | −43130/3 | 505465/6 | −1579685/6 |
| $V_6$ | −270 | 18730 | −236957.5 | 1324138.7 |
| $V_7$ | | −35840/3 | 1127735/3 | −58375583/15 |
| $V_8$ | | 8960/3 | −1020215/3 | 21159859/3 |
| $V_9$ | | | 164062.5 | −8005336.5 |
| $V_{10}$ | | | −32812.5 | 5552830.5 |
| $V_{11}$ | | | | −2155507.2 |
| $V_{12}$ | | | | 359251.2 |

## IV. NUMERICAL EXAMPLES

To verify the analysis presented in previous sections, various problems will be considered. These problems are assumed to belong to a system governed by equation (1), with coefficients $\kappa_{ij}(\mathbf{x})$ and $\psi(\mathbf{x})$ of the form (4) and (5), respectively, and satisfying the initial condition (3) and specific boundary conditions as discussed in Section II. The coefficients may represent properties such as diffusivity, conductivity, or change rate of the dependent variable $T(\mathbf{x},t)$. The solutions will be obtained numerically using standard boundary element method (BEM) with constant elements, with a unit square as the geometrical domain and a time interval of $0 \leq t \leq 5$. The FORTRAN programming language will be used, with a script developed to calculate the solutions and measure the CPU time for obtaining them. Another script is also included to calculate the values of coefficients $V_m$, which are listed in Table I for various even values of $N$. The problems considered may have analytical solutions or may not, but all will be governed by equation (1) and will have the characteristics described by the coefficients.

For all problems the inhomogeneity function is taken to be

$$\begin{aligned} g^{1/2}(\mathbf{x}) &= \cos(1 - 0.25x_1 - 0.75x_2) \\ &\quad + \sin(1 - 0.25x_1 - 0.75x_2) \end{aligned}$$

and the constant anisotropy coefficient $\overline{\kappa}_{ij}$

$$\overline{\kappa}_{ij} = \begin{bmatrix} 1 & 0.25 \\ 0.25 & 0.9 \end{bmatrix}$$

so that (7) implies

$$\lambda = -0.6625$$

### A. Examples with analytical solutions

*1) Problem 1::* Other aspects that will be justified are the convergence (as $N$ increases) and time efficiency for obtaining the numerical solutions. The analytical solutions are assumed to take a separable variables form

$$T(\mathbf{x},t) = g^{-1/2}(\mathbf{x})\,h(\mathbf{x})\,f(t)$$

where $h(\mathbf{x}), f(t)$ are continuous functions. The boundary conditions are assumed to be (see Figure 1)

$P$ is given on side AB
$P$ is given on side BC
$T$ is given on side CD
$P$ is given on side AD

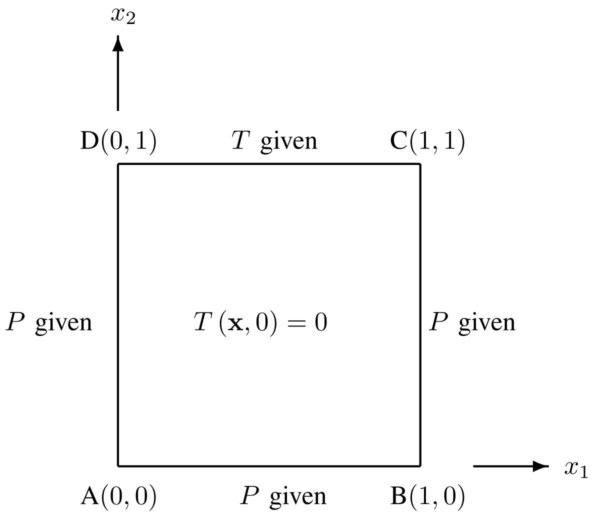


Fig. 1. The boundary conditions for the problems in Section IV-A

For each $N$, numerical solutions for $T$ and the derivatives $\partial T/\partial x_1$ and $\partial T/\partial x_2$ at $19\times 19$ points inside the space domain which are

$$\begin{aligned}(x_1,x_2) &= \{0.05,0.1,0.15,\ldots,0.9,0.95\} \\ &\quad\times\{0.05,0.1,0.15,\ldots,0.9,0.95\}\end{aligned}$$

and 11 time-steps which are

$$t=0.0005,0.5,1,1.5,\ldots,4,4.5,5$$

are computed. The aggregate relative error $E$ is calculated using the norm

$$E=\left[\frac{\sum_t\sum_{i=1}^{19\times 19}\left(\varsigma_{n,i}-\varsigma_{a,i}\right)^2}{\sum_t\sum_{i=1}^{19\times 19}T_{a,i}^2}\right]^{\frac{1}{2}}$$

where $\varsigma_n$ and $\varsigma_a$ represent respectively the numerical and analytical solutions $T$ or the derivatives $T_1=\partial T/\partial x_1$ and $T_2=\partial T/\partial x_2$. The elapsed CPU time $\tau$ (in seconds) is also computed and the time efficiency number $e$ for obtaining the numerical solutions of error $E$ is defined as

$$e=E\tau$$

This formula explains that the smaller time $\tau$ with smaller error $E$, the more efficient the procedure (smaller $e$).

*Case 1::* We take

$$\begin{aligned}h(\mathbf{x}) &= 1-0.45x_1-0.55x_2 \\ f(t) &= 1-\exp(-1.75t)\end{aligned}$$

Thus for $h(\mathbf{x})$ to satisfy (15)

$$\overline{\psi}=0.6625/s$$

Table II shows the error $E$ and efficiency number $e$ for solutions $T,\partial T/\partial x_1,\partial T/\partial x_2$ as $N$ increases from $N=6$ to $N=12$. For the solutions $T,\partial T/\partial x_1,\partial T/\partial x_2$ the error $E$ gets smaller as $N$ moves up to $N=12$, but the efficiency number $e$ decreases as $N$ moves up to $N=10$.

Therefore as shown in Table III, the optimized value of $N$ for solutions $T,\partial T/\partial x_1,\partial T/\partial x_2$ to achieve their smallest error $E$ is $N=12$, but to reach their smallest efficiency number $e$ the optimized value of $N$ is $N=10$.

In addition Figure 2 shows the numerical and analytical solutions $T$, $\partial T/\partial x_1$ and $\partial T/\partial x_2$ at $(x_1,x_2)=(0.5,0.5)$.

TABLE II
THE TOTAL ELAPSED CPU TIME $\tau$, THE GLOBAL AVERAGE ERROR $E$, THE EFFICIENCY NUMBER $e=\tau E$ FOR CASE 1

| $N$ | | 6 | 8 | 10 | 12 |
|---|---|---|---|---|---|
| $\tau$ | | 368.844 | 489.328 | 611.984 | 765.375 |
| $T$ | $E$ | 0.00430905 | 0.00134085 | 0.00056592 | 0.00054383 |
| | $e$ | 1.589366 | 0.656117 | 0.346335 | 0.416230 |
| $\frac{\partial T}{\partial x_1}$ | $E$ | 0.00414985 | 0.00126870 | 0.00048291 | 0.00040641 |
| | $e$ | 1.530645 | 0.620811 | 0.295534 | 0.311058 |
| $\frac{\partial T}{\partial x_2}$ | $E$ | 0.00418428 | 0.00127630 | 0.00048001 | 0.00041348 |
| | $e$ | 1.543345 | 0.624530 | 0.293761 | 0.316464 |

TABLE III
THE OPTIMIZED VALUE OF $N$ FOR OBTAINING THE NUMERICAL SOLUTIONS $T,\partial T/\partial x_1,\partial T/\partial x_2$ OF BEST ERROR $E$ AND EFFICIENCY NUMBER $e$ FOR CASE 1

| | $T$ | $\frac{\partial T}{\partial x_1}$ | $\frac{\partial T}{\partial x_2}$ |
|---|---|---|---|
| $E$ | $N=12$ | $N=12$ | $N=12$ |
| $e$ | $N=10$ | $N=10$ | $N=10$ |

*Case 2::* For the analytical solution we take

$$\begin{aligned}h(\mathbf{x}) &= \cos(1-0.45x_1-0.55x_2) \\ f(t) &= t/5\end{aligned}$$

So that in order for $h(\mathbf{x})$ to satisfy (15)

$$\overline{\psi}=0.064/s$$

Tables IV and V show that for solution $T$ the smallest error $E$ and efficiency number $e$ are achieved when $N=12$, whereas for the solutions $\partial T/\partial x_1,\partial T/\partial x_2$ they are reached when $N=8$. According to Hassanzadeh and Pooladi-Darvish [24] increasing $N$ will increase the accuracy up to a point, and then the accuracy will decline due to round-off errors. Figure 3 shows the numerical and analytical solutions $T$, $\partial T/\partial x_1$ and $\partial T/\partial x_2$ at $(x_1,x_2)=(0.5,0.5)$.

*Case 3::* We take

$$\begin{aligned}h(\mathbf{x}) &= \exp(-1+0.45x_1+0.55x_2) \\ f(t) &= 0.16t(5-t)\end{aligned}$$

Therefore (15) gives

$$\overline{\psi}=1.261/s$$

TABLE IV
THE TOTAL ELAPSED CPU TIME $\tau$, THE GLOBAL AVERAGE ERROR $E$, THE EFFICIENCY NUMBER $e=\tau E$ FOR CASE 2

| $N$ | | 6 | 8 | 10 | 12 |
|---|---|---|---|---|---|
| $\tau$ | | 554.969 | 740.016 | 905.547 | 996.891 |
| $T$ | $E$ | 0.00189257 | 0.00042125 | 0.00030997 | 0.00026982 |
| | $e$ | 1.050319 | 0.311732 | 0.280693 | 0.268981 |
| $\frac{\partial T}{\partial x_1}$ | $E$ | 0.00236961 | 0.00052920 | 0.00055832 | 0.00080585 |
| | $e$ | 1.315062 | 0.391613 | 0.505587 | 0.803342 |
| $\frac{\partial T}{\partial x_2}$ | $E$ | 0.00275614 | 0.00051205 | 0.00062512 | 0.00071689 |
| | $e$ | 1.529572 | 0.378922 | 0.566073 | 0.714661 |

TABLE V
THE OPTIMIZED VALUE OF $N$ FOR OBTAINING THE NUMERICAL SOLUTIONS $T,\partial T/\partial x_1,\partial T/\partial x_2$ OF BEST ERROR $E$ AND EFFICIENCY NUMBER $e$ FOR CASE 2

| | $T$ | $\frac{\partial T}{\partial x_1}$ | $\frac{\partial T}{\partial x_2}$ |
|---|---|---|---|
| $E$ | $N=12$ | $N=8$ | $N=8$ |
| $e$ | $N=12$ | $N=8$ | $N=8$ |

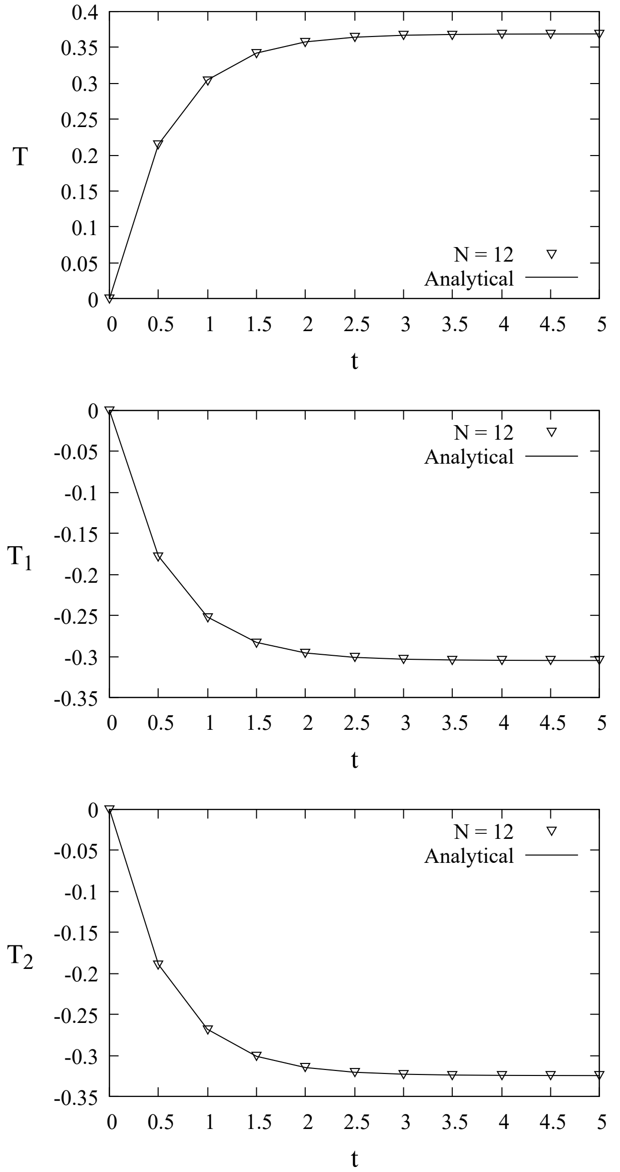


Fig. 2. The solutions $T$, $\partial T/\partial x_1$ and $\partial T/\partial x_2$ at $(x_1, x_2) = (0.5, 0.5)$ of $N = 12$ for Case 1.

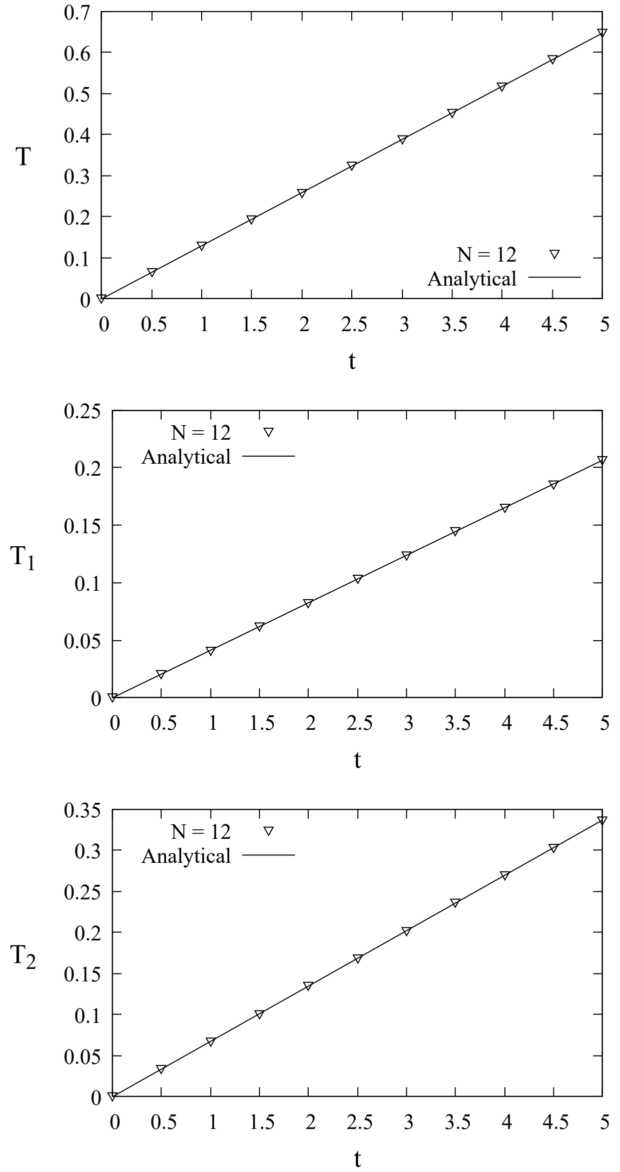


Fig. 3. The solutions $T$, $\partial T/\partial x_1$ and $\partial T/\partial x_2$ at $(x_1, x_2) = (0.5, 0.5)$ of $N = 12$ for Case 2

TABLE VI
THE TOTAL ELAPSED CPU TIME $\tau$, THE GLOBAL AVERAGE ERROR $E$, THE EFFICIENCY NUMBER $e = \tau E$ FOR CASE 3

| $N$ | | 6 | 8 | 10 | 12 |
|---|---|---|---|---|---|
| $\tau$ | | 322.031 | 429.984 | 537.766 | 646.359 |
| $T$ | $E$ | 0.16850814 | 0.01081065 | 0.00051311 | 0.00039817 |
| | $e$ | 54.264887 | 4.648411 | 0.275932 | 0.257358 |
| $\frac{\partial T}{\partial x_1}$ | $E$ | 0.16861177 | 0.01095677 | 0.00049441 | 0.00055541 |
| | $e$ | 54.298260 | 4.711238 | 0.265878 | 0.358997 |
| $\frac{\partial T}{\partial x_2}$ | $E$ | 0.16862487 | 0.01096944 | 0.00033486 | 0.00032938 |
| | $e$ | 54.302479 | 4.716689 | 0.180078 | 0.212899 |

Tables VI and VII show that for solutions $T$ the smallest error $E$ and efficiency number $e$ are achieved when $N = 12$, for solutions $\partial T/\partial x_1$ the smallest error $E$ and efficiency number $e$ are achieved when $N = 10$, whereas for the solutions $\partial T/\partial x_2$ they are reached when $N = 12$ and $N = 10$ respectively. Meanwhile, Figure 4 shows the numerical and analytical solutions $T$, $\partial T/\partial x_1$ and $\partial T/\partial x_2$ at $(x_1, x_2) = (0.5, 0.5)$.

TABLE VII
THE OPTIMIZED VALUE OF $N$ FOR OBTAINING THE NUMERICAL SOLUTIONS $T, \partial T/\partial x_1, \partial T/\partial x_2$ OF BEST ERROR $E$ AND EFFICIENCY NUMBER $e$ FOR CASE 3

| | $T$ | $\frac{\partial T}{\partial x_1}$ | $\frac{\partial T}{\partial x_2}$ |
|---|---|---|---|
| $E$ | $N = 12$ | $N = 10$ | $N = 12$ |
| $e$ | $N = 12$ | $N = 10$ | $N = 10$ |

### B. Examples without analytical solutions

The aim is to show the effect of inhomogeneity and anisotropy of the considered material on the solution $T$.

*1) Problem 2::* The material is supposed to be either inhomogeneous or homogeneous and either anisotropic or isotropic. If the material is homogeneous then

$$g(\mathbf{x}) = 1$$

and if it is isotropic then

$$\overline{\kappa}_{ij} = \begin{bmatrix} 1 & 0 \\ 0 & 1 \end{bmatrix}$$

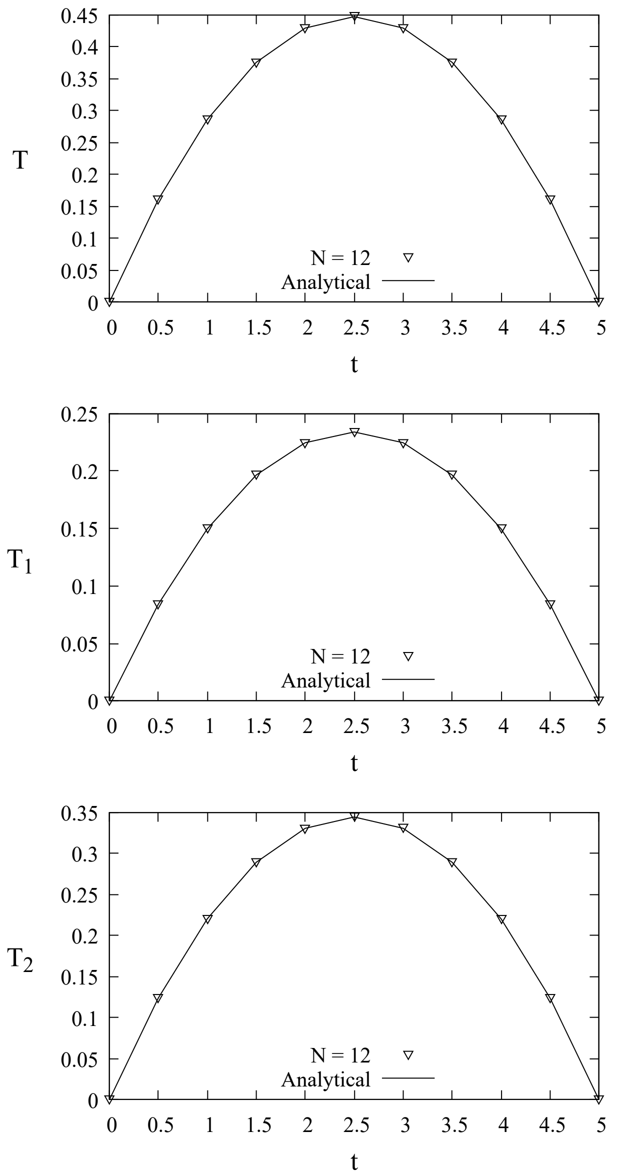


Fig. 4. The solutions $T$, $\partial T/\partial x_1$ and $\partial T/\partial x_2$ at $(x_1, x_2) = (0.5, 0.5)$ of $N = 12$ for Case 3

So that there are four cases regarding the material, namely anisotropic inhomogeneous, anisotropic homogeneous, isotropic inhomogeneous and isotropic homogeneous material. We set $\overline{\psi} = 1$ and the boundary conditions are (see Figure 5)

$$\begin{array}{l} P = P(t) \text{ on side AB} \\ P = 0 \text{ on side BC} \\ T = 0 \text{ on side CD} \\ P = 0 \text{ on side AD} \end{array}$$

where $P(t)$ takes four forms

$$\begin{aligned} P(t) = P_1(t) &= 1 \\ P(t) = P_2(t) &= 1 - \exp(-1.75t) \\ P(t) = P_3(t) &= t/5 \\ P(t) = P_4(t) &= 0.16t(5 - t) \end{aligned}$$

Therefore the system is geometrically symmetric about $x_1 = 0.5$. We use $N = 12$ for all cases of this problem.

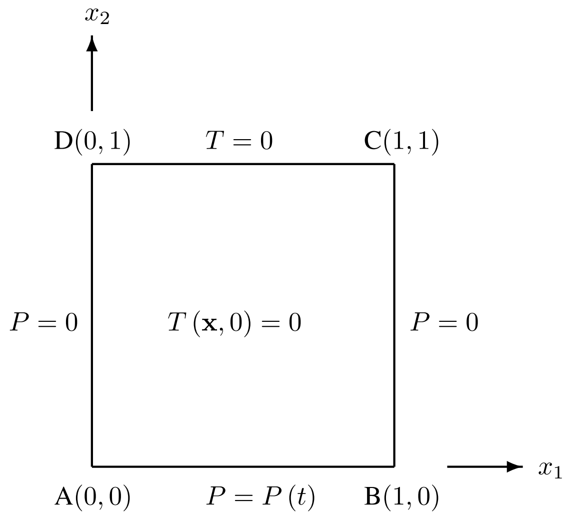


Fig. 5. The boundary conditions for Problem 2.

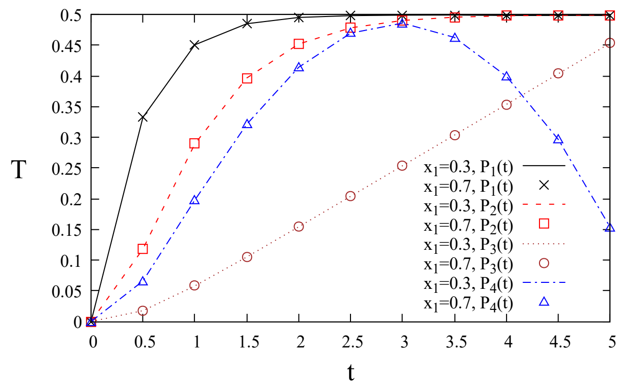


Fig. 6. Solution $T$ at points $(0.2, 0.5)$ , $(0.8, 0.5)$ for Problem 2 of isotropic homogeneous material.

The results are shown in Figures 6, 7 and 8. Figure 6 depicts solution $T$ at points $(0.3, 0.5)$ , $(0.7, 0.5)$ when the material under consideration is an isotropic homogeneous material. It can be seen that the values of $T$ at point $(0.3, 0.5)$ coincide with those at point $(0.7, 0.5)$. This is to be expected as the system is symmetrical about $x_1 = 0.5$ when the material is isotropic homogeneous. However, if the material is anisotropic homogeneous the values of $T$ at point $(0.3, 0.5)$ do not coincide with those at point $(0.7, 0.5)$. See Figure 7. This means anisotropy gives effect on the values of $T$. Similarly, if the material is isotropic inhomogeneous (see Figure 8) the values of $T$ at point $(0.3, 0.5)$ differ from those at point $(0.7, 0.5)$. This indicates that inhomogeneity also gives effect on the values of $T$.

In addition, Figures 6, 7 and 8 show that the trends of $T$ values (as the time $t$ changes) follow the time variation of $P(t)$ except for the form of $P(t) = 1$. This is to be expected as $P(t)$, acting as the boundary condition on side AB, is the only time-dependent quantity for the system, and the coefficients $\kappa_{ij}(\mathbf{x}), \psi(\mathbf{x})$ are time independent. Moreover, as shown in Figures 6 and 8, it is also expected that the values of $T$ for the cases of $P_1(t) = 1$ and $P_2(t) = 1 - \exp(-1.75t)$ tend to approach same steady state solution as $t$ increases. Both functions $P_1(t) = 1$ and $P_2(t) = 1 - \exp(-1.75t)$ will converge to 1 as $t$ gets bigger.

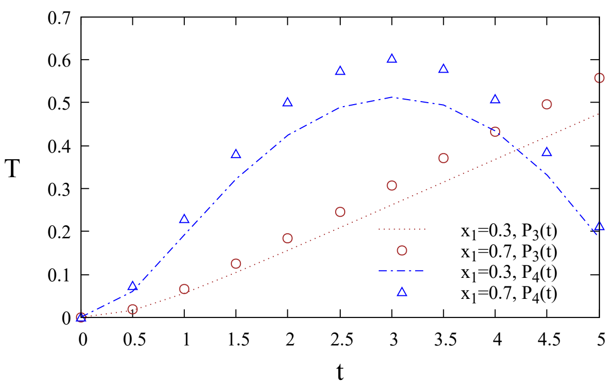


Fig. 7. Solution $T$ at points $(0.2, 0.5)$ , $(0.8, 0.5)$ for Problem 2 of anisotropic homogeneous material.

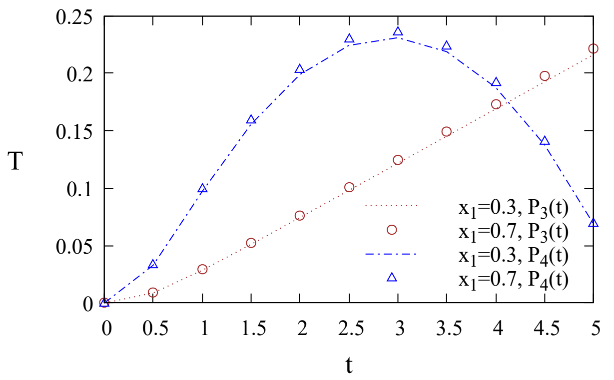


Fig. 8. Solution $T$ at points $(0.2, 0.5)$ , $(0.8, 0.5)$ for Problem 2 of isotropic inhomogeneous material.

## V. Conclusion

The Laplace transform and standard boundary element method (BEM) have been combined to find numerical solutions for initial boundary value problems for anisotropic trigonometrically graded materials governed by the Laplace equation. This method is simple to implement and accurate because it does not involve a fundamental solution with singular time points and thus avoids round-off error propagation. To use the boundary integral equation, the values of the boundary conditions in time variable $t$ must be Laplace transformed first. This means that the initial boundary conditions are actually approximations from the beginning, making it crucial to use an accurate numerical Laplace transform inversion technique. The Stehfest formula has been found to be quite accurate based on the results of problems in the Examples with Analytical Solutions section. The Laplace transform and standard BEM have been applied to a class of trigonometrically graded materials where the coefficients depend on the spatial variable only with the same inhomogeneity or gradation function. It would be interesting to extend this study to cases where the coefficients depend on different gradation functions that vary with the time variable.

## References


[1] Y. C. Shiah, Y-C. Chaing, T. Matsumoto, "Analytical transformation of volume integral for the time-stepping BEM analysis of 2D transient heat conduction in anisotropic media," *Engineering Analysis with Boundary Elements*, vol. 64, pp. 101–110, 2016.

[2] Q. Li, S. Chen, X. Luo, "Steady heat conduction analyses using an interpolating element-free Galerkin scaled boundary method," *Applied Mathematics and Computation*, vol. 300, pp. 103–115, 2017.

[3] K. Yang, W-z. Feng, J. Wang, X-w. Gao, "RIBEM for 2D and 3D nonlinear heat conduction with temperature dependent conductivity," *Engineering Analysis with Boundary Elements*, vol. 87, pp. 1–8, 2018.

[4] S.Y. Reutskiy, "A meshless radial basis function method for 2D steady-state heat conduction problems in anisotropic and inhomogeneous media," *Engineering Analysis with Boundary Elements*, vol. 66, 1–11, 2016.

[5] S. Abotula, A. Kidane, V.B. Chalivendra, A. Shukla, "Dynamic curving cracks in functionally graded materials under thermo-mechanical loading," *International Journal of Solids and Structures*, vol. 49, 1637, 2012.

[6] H. Abadikhah, P.D. Folkow, "Dynamic equations for solid isotropic radially functionally graded circular cylinders," *Composite Structures*, vol. 195, 147, 2018.

[7] S. Guo, J. Zhang, G. Li, F. Zhou, "Three-dimensional transient heat conduction analysis by Laplace transformation and multiple reciprocity boundary face method," *Engineering Analysis with Boundary Elements*, vol. 37, pp. 15, 2013.

[8] Z. Fu, J. Shi, W. Chen, L. Yang, "Three-dimensional transient heat conduction analysis by boundary knot method," *Mathematics and Computers in Simulation*, vol. 165, pp. 306–317, 2019.

[9] Y. Chen, Q. Du, "Some Fast Algorithms for Exterior Anisotropic Problems in Concave Angle Domains," *IAENG International Journal of Applied Mathematics*, vol. 50, no.4, pp. 729–733, 2020.

[10] W. Timpitak, N. Pochai, "Numerical Simulations to a One-dimensional Groundwater Pollution Measurement Model Through Heterogeneous Soil," *IAENG International Journal of Applied Mathematics*, vol. 50, no.3, pp. 558–565, 2020.

[11] N. Noda, N. Sumi, M. Ohmichi, "Analysis of transient plane thermal stresses in functionally graded orthotropic strip," *Journal of Thermal Stresses*, vol. 41, pp. 1225–1243, 2018.

[12] M. I. Azis, D. L. Clements, "Nonlinear transient heat conduction problems for a class of inhomogeneous anisotropic materials by BEM," *Engineering Analysis with Boundary Elements*, vol. 32, pp. 1054–1060, 2008.

[13] N. Samec, L. Škerget, "Integral formulation of a diffusive–convective transport equation for reacting flows," *Engineering Analysis with Boundary Elements*, vol. 28, pp. 1055–1060, 2004.

[14] J. Ravnik, L. Škerget, "A gradient free integral equation for diffusion–convection equation with variable coefficient and velocity," *Engineering Analysis with Boundary Elements*, vol. 37, pp. 683–690, 2013.

[15] J. Ravnik, L. Škerget, "Integral equation formulation of an unsteady diffusion–convection equation with variable coefficient and velocity," *Computers and Mathematics with Applications*, vol. 66, pp. 2477–2488, 2014.

[16] S. A. AL-Bayati, L. C. Wrobel, "A novel dual reciprocity boundary element formulation for two-dimensional transient convection–diffusion–reaction problems with variable velocity," *Engineering Analysis with Boundary Elements*, vol. 94, pp. 60–68, 2018.

[17] S. A. AL-Bayati, L. C. Wrobel, "The dual reciprocity boundary element formulation for convection-diffusion-reaction problems with variable velocity field using different radial basis functions," *International Journal of Mechanical Sciences*, vol. 145, pp. 367–377, 2018.

[18] J. Ravnik, J. Tibuat, "Fast boundary-domain integral method for unsteady convection-diffusion equation with variable diffusivity using the modified Helmholtz fundamental solution," *Numerical Algorithms*, vol. 82, pp. 1441–1466, 2019.

[19] M. I. Azis, "Numerical solutions for the Helmholtz boundary value problems of anisotropic homogeneous media," *Journal of Computational Physics*, vol. 381, pp. 42–51, 2019.

[20] M. I. Azis, I. Solekhudin, M. H. Aswad, A. R. Jalil, "Numerical simulation of two-dimensional modified Helmholtz problems for anisotropic functionally graded materials," *Journal of King Saud University - Science*. vol. 32, no. 3, pp. 2096–2102, 2020.

[21] M. A. H. Assagaf, A. Massinai, A. Ribal, S. Toaha, M. I. Azis, "Numerical simulation for steady anisotropic-diffusion convection problems of compressible flow in exponentially graded media," *Journal of Physics: Conference Series*, vol. 1341, no. 8, 082016, 2019.

[22] N. Salam, A. Haddade, D. L. Clements, M. I. Azis, "A boundary element method for a class of elliptic boundary value problems of functionally graded media," *Engineering Analysis with Boundary Elements*, vol. 84, pp. 186–190, 2017.

[23] M. I. Azis, "Standard-BEM solutions to two types of anisotropic-diffusion convection reaction equations with variable coefficients," *Engineering Analysis with Boundary Elements*, vol. 105, pp. 87–93, 2019.

[24] H. Hassanzadeh, M. Pooladi-Darvish, "Comparison of different numerical Laplace inversion methods for engineering applications," *Appl. Math. Comput.*, vol. 189, pp. 1966–1981, 2007.